Mouse Models of Tumor Development in Neurofibromatosis Type 1

Karen Cichowski *et al.*

Science **286**, 2172 (1999);
DOI: 10.1126/science.286.5447.2172

Science (print ISSN 0036-8075; online ISSN 1095-9203) is published weekly, except the last week in December, by the American Association for the Advancement of Science, 1200 New York Avenue NW, Washington, DC 20005.

corneas (Fig. 4, D to F). These results showed that the corneal equivalents had an active response to different grades of injury, an important functional characteristic of human corneas.

These engineered corneal equivalents have immediate applications as human ocular irritancy models for evaluating new chemicals and drugs, as alternatives to animals (*30*), and in drug efficacy testing such as for wound healing. The corneal equivalents can also be used in biomedical research, for example, to study wound healing and cell-matrix interactions. This technology provides a strong basis for the development of temporary or permanent cornea replacements with low rejection rates. Future research could lead to readily available, complex engineered tissues that reproduce their natural human counterparts and are suitable for implants, transplants, and biomedical research.

References and Notes

1. D. G. Pitts, in *Environmental Vision*, D. E. Pitts and R. N. Kleinstein, Eds. (Butterworth-Heinemann, Boston, 1994), chap. 6.
2. M. J. Jager *et al.*, *Eye* **9**, 241 (1995).
3. Y. Minami, H. Sugihara, S. Oono, *Invest. Ophthalmol. Visual Sci.* **34**, 2316 (1993); J. D. Zieske *et al.*, *Exp. Cell Res.* **214**, 621 (1994); C. R. Kahn, E. Young, I. H. Lee, J. S. Rhim, *Invest. Ophthalmol. Visual Sci.* **34**, 1983 (1993); K. Araki-Sasaki *et al.*, *Invest. Ophthalmol. Visual Sci.* **36**, 614 (1995); L. Germain *et al.*, *Pathobiology* **67**, 140 (1999).
4. "Immortalized cells" are cells with extended lifespans that retain characteristics of low-passage or freshly dissociated cells (contact inhibition, substrate-dependent growth, but no senescence or culture-related phenotypic changes after 8 to 10 passages).
5. C. L. Halbert, G. W. Demers, D. A. Galloway, *J. Virol.* **65**, 473 (1991); *J. Virol.* **66**, 2125 (1992). Viral producer cell line PA317LXSN 16E6E7 (American Type Culture Collection) was used.
6. J. S. Rhim *et al.*, *Carcinogenesis* **19**, 673 (1998).
7. R. E. Kingston, in *Current Protocols Molecular Biology*, F. M. Ausubel *et al.*, Eds. (Wiley, New York, 1997), pp. 9.0.1–9.1.11.
8. T. M. Bryan and R. R. Reddel, *Crit. Rev. Oncog.* **5**, 331 (1994); P. J. Southern and P. Berg, *J. Mol. Appl. Genet.* **1**, 327 (1982).
9. F. L. Graham and A. J. van der Eb, *Virology* **52**, 456 (1973); M. P. Quinlan, *Oncogene* **9**, 2639 (1994).
10. Cytogenetic analyses were performed by H. S. Wang (Cytogenetics Laboratory, Children's Hospital of Eastern Ontario, Ottawa) using routine G-banding techniques with 400- to 450-band resolution.
11. M. J. Pettenati *et al.*, *Hum. Genet.* **101**, 26 (1997).
12. TeloQuant Telomeric Repeat Amplification Protocol kit (Pharmingen Canada).
13. J. L. Rae, K. E. Cooper, P. Gates, M. A. Watsky, *Br. J. Neurosci. Methods* **37**, 15 (1991).
14. C. Bockman, C. M. Griffith, M. A. Watsky, *Invest. Ophthalmol. Visual Sci.* **39**, 1143 (1998).
15. Epithelial cells showed corneal epithelial-specific keratin 12 staining [A. Schermer, S. Galvin, T. T. Sun, *J. Cell Biol.* **103**, 49 (1986)] with AE5 antibody (ICN Biochemicals, Aurora, OH). Stromal cells stained for vimentin (Roche Diagnostics, Montreal). Endothelial cells expressed α2(VIII) collagen mRNA [Y. Muragaki *et al.*, *J. Biol. Chem.* **266**, 7721 (1991)] and lacked keratin 12 staining.
16. E. Bell, H. P. Ehrlich, D. J. Buttle, T. Nakatsuji, *Science* **211**, 1052 (1981); M. S. Shoichet and J. A. Hubell, Eds., *Polymers for Tissue Engineering* (VSP, Utrecht, Netherlands, 1998).
17. Cell lines producing successful constructs were from young donors, were immortalized with HPV E6/E7, and had appropriate electrophysiological responses.
18. M. Griffith *et al.*, in preparation.
19. W. W. Y. Kao, R. A. Berg, D. J. Prockop, *Biochim. Biophys. Acta* **411**, 202 (1975); C. J. Doillon, F. H. Silver, R. A. Berg, *Biomaterials* **8**, 195 (1987).
20. M. Griffith *et al.*, unpublished data.
21. R. Janvier, A. Sourla, M. Koutsilieris, C. J. Doillon, *Anticancer Res.* **17**, 1551 (1997).
22. M. A. Watsky, T. W. Olsen, H. F. Edelhauser, in *Duane's Foundations of Clinical Ophthalmology*, B. Tasman and E. Jaeger, Eds. (Lippincott, Philadelphia, 1995), vol. 2, chap. 4.
23. D. H. Geroski, J. C. Kies, and H. F. Edelhauser [*Curr. Eye Res.* **3**, 331 (1984)] showed that 100 μM ouabain causes swelling of human corneas (41 μm per hour); after 2 hours corneas would swell by 82 μm (16%).
24. Constructs, with epithelium sealed with silicone oil to prevent movement of water across the anterior surface, were measured using OCT (Zeiss-Humphrey, San Leandro, CA). The average change in thickness was calculated from four to six measurements before and after treatment of the endothelial surface for 2 hours with 100 μM ouabain or Dulbecco's modified Eagle's medium alone (DMEM, Gibco).
25. Corneal equivalents and human eye bank corneas were treated with 5% SDS or medium 199 alone (controls) for 3 min. After a 1-hour recovery period, total RNA was extracted and mRNA was reverse-transcribed. Specific cDNA was amplified by PCR using *Taq* polymerase (Gibco) and primer pairs specific for human nucleotide sequences [for c-*fos*, sense (S): 5′-CTTCAACGCAGACTACGAGG, antisense (A): 5′-CTGTCATGGTCTTCACAACG; for IL-1α, S: 5′-ATCCTGAATGACGCCCTCAA, A: 5′-GGATGGGCAACTGATGTGAA; for IL-6, S: 5′-AATTCGGTACATCCTCGACG, A: 5′-GCGCAGAATGAGATGAGTTG; for bFGF (*FGF-2*), S: 5′-GAGAAGAGCGACCCTCACA, A: 5′-TAGCTTTCTGCCCAGGTCC; for VEGF, S: 5′-ACTTTCTGCTGTCTTGGGTG, A: 5′-TGCTGTAGGAAGCTCATCTC; for Coll I, S: 5′-GGTGATGCTGGTCCTGTT, A: 5′-GTCCTTGGGGTTCTTGCT]. 18*S* rRNA primers and Competimers (QuantumRNA 18 Internal Standards Kit; Ambion, Austin, TX) were introduced into the PCR mixture and 18*S* RNA was amplified together with the gene-specific cDNA and primers, within the linear amplification range, to provide internal standards for quantifying relative differences in gene expression [W. C. Gause and J. Adamovicz, in *PCR Primer: A Laboratory Manual*, C. W. Dieffenbach, Ed. (Cold Spring Harbor Laboratory Press, Plainview, NY, 1995)]. PCR products were sequenced to confirm identities. To increase the sensitivity, we transferred PCR products separated by agarose gel electrophoresis to Southern (DNA) blot substrate and hybridized them with [^{32}P]deoxycytidine triphosphate–labeled specific probes. Quantification was performed on a Molecular Dynamics Storm Phosphorimager.
26. J. H. Draize, G. Woodard, H. O. Calvery, *J. Pharmacol. Exp. Ther.* **82**, 377 (1944); J. F. Griffith, G. A. Nixon, R. D. Bruce, P. J. Reer, E. A. Bannan, *Toxicol. Appl. Pharmacol.* **55**, 501 (1980).
27. c-*fos*: Y. Okada *et al.*, *Graefes Arch. Clin. Exp. Ophthalmol.* **236**, 853 (1998); IL-1 and IL-6: C. Sotozono *et al.*, *Curr. Eye Res.* **16**, 670 (1997); bFGF: V. P. T. Hoppenreijs, E. Pels, G. F. J. M. Vrensen, W. F. Treffers, *Invest. Ophthalmol. Visual Sci.* **35**, 931 (1994); VEGF: S. Amano, R. Roban, M. Kuroki, M. Tolentino, A. P. Adamis, *Invest. Ophthalmol. Visual Sci.* **39**, 18 (1998); Coll I: W. J. Power, A. H. Kaufman, J. Merayo-Lloves, V. Arrunategui-Correa, C. S. Foster, *Curr. Eye Res.* **14**, 879 (1995).
28. Live/Dead Viability/Cytotoxicity kit (Molecular Probes, Eugene, OR).
29. Corneal equivalents, rabbit corneas (PelFreez, Rogers, AR), and human eye bank corneas 1 to 4 weeks post-enucleation (Eye Bank of Canada, Toronto) were treated with 100 μl of coded test substance for 5 min, then rinsed with phosphate-buffered saline. Transmission measurements were made with a custom-built instrument [D. Priest and R. Munger, *Invest. Ophthalmol. Visual Sci.* **39**, S352 (1998)] before (T_1) and after (T_2) chemical exposure. Responses were plotted as normalized change in transmission, $CT_n = [(T_1 - T_2)/T_2] \times 100$, and compared within and across species using analysis of variance (ANOVA).
30. International Life Sciences Institute, *J. Toxicol. Cutaneous Ocul. Toxicol.* **15**, 211 (1996).

31. Supported by grants from the Natural Sciences and Engineering Research Council of Canada, Medical Research Council–Pharmaceutical Manufacturers' Association of Canada, and the P&G International Program for Animal Alternatives. We thank S. Whelan and P. Berg for Ad5 and psv3neo plasmids, C. Smith and Ottawa Hospital Research Institute colleagues, and E. Hay and A. Tashjian Jr. for helpful insights during preparation of this manuscript.

27 August 1999; accepted 4 November 1999

Mouse Models of Tumor Development in Neurofibromatosis Type 1

Karen Cichowski,[1]* T. Shane Shih,[1,2]* Earlene Schmitt,[1,3] Sabrina Santiago,[1] Karlyne Reilly,[1] Margaret E. McLaughlin,[4] Roderick T. Bronson,[5] Tyler Jacks[1,6]†

Neurofibromatosis type 1 (NF1) is a prevalent familial cancer syndrome resulting from germ line mutations in the *NF1* tumor suppressor gene. Hallmark features of the disease are the development of benign peripheral nerve sheath tumors (neurofibromas), which can progress to malignancy. Unlike humans, mice that are heterozygous for a mutation in *Nf1* do not develop neurofibromas. However, as described here, chimeric mice composed in part of *Nf1*$^{-/-}$ cells do, which demonstrates that loss of the wild-type *Nf1* allele is rate-limiting in tumor formation. In addition, mice that carry linked germ line mutations in *Nf1* and *p53* develop malignant peripheral nerve sheath tumors (MPNSTs), which supports a cooperative and causal role for p53 mutations in MPNST development. These two mouse models provide the means to address fundamental aspects of disease development and to test therapeutic strategies.

Neurofibromatosis type I (NF1) affects about 1 in 3500 individuals worldwide (*1*). The hallmark clinical feature of the disease is development of multiple benign neurofibromas, which can be debilitating, severely disfiguring, and, in some patients, progress to

malignancy (*2*). NF1 patients are also predisposed to developing optic pathway gliomas, pheochromocytomas, and myeloid leukemia as well as several symptoms unrelated to cancer (*3*).

The *NF1*-encoded protein neurofibromin is a member of the GTPase-activating protein (GAP) family that includes mammalian $p120^{GAP}$ and the yeast IRA proteins (*4*). Like $p120^{GAP}$, neurofibromin can stimulate the GTPase activity of Ras in vitro and in vivo (*5*). Because most mutations in the *NF1* gene in patients are predicted to result in loss of function, deregulation of Ras-mediated signaling is likely to contribute to the pathology of NF1 (*6*).

Although *NF1* appears to be a classic tumor suppressor gene, the molecular mechanism underlying tumor development in NF1 has been obscure. Although second hit mutations affecting the inherited wild-type *NF1* allele have been clearly identified in the myeloid leukemias and pheochromocytomas in NF1 patients (*7*), such mutations have been reported for only a small number of neurofibromas (*8*). The difficulty in detecting mutations may be due in part to the complex nature of these lesions, which are composed of multiple cell types, not all of which are expected to develop a second mutation (*2*). However, it also has been suggested that *NF1* heterozygosity may be sufficient for development of benign neurofibromas (haplo-insufficiency), with full loss of *NF1* function being restricted to the progression to MPNSTs (*9*).

Heterozygous mutant ($Nf1^{+/-}$) animals are predisposed to a number of tumor types; however, they do not develop peripheral nerve sheath tumors or other characteristic symptoms of human NF1 (*10, 11*). To test the possibility that a mutation in the wild-type *Nf1* allele is required and rate-limiting in the formation of neurofibromas in $Nf1^{+/-}$ mice, we generated chimeric mice that were partially composed of $Nf1^{-/-}$ cells. Germ line homozygosity for a *Nf1* mutation ($Nf1^{-/-}$) results in embryonic lethality at about day 14 of gestation (*10, 11*). We also developed a model of MPNST formation by generating mice with combined mutations in *Nf1* and *p53*. These two models are described below.

We created two *Nf1*-deficient embryonic stem cell (ES) lines by successive rounds of gene targeting and injected the cells into C57BL/6 blastocysts to generate chimeric mice (*12*). We analyzed 18 chimeric adults, which fell into three phenotypic classes, in this study (*13*). The subset of chimeras (n = 4) that exhibited the highest degree of chimerism died by 1 month of age of unknown causes. The two animals that exhibited the lowest degree of chimerism (less than 15% by coat color) lived a typical life span and no unusual pathology was observed upon necropsy. Most animals (12/18) fell into the third phenotypic class: they exhibited a moderate degree of chimerism, frequent myelodysplasia, and progressive neuromotor defects. The life span of these animals varied from 2 to 26 months. Histological analysis of this subset of mice revealed the presence of neurofibromas in every animal (*14*). We detected mul-

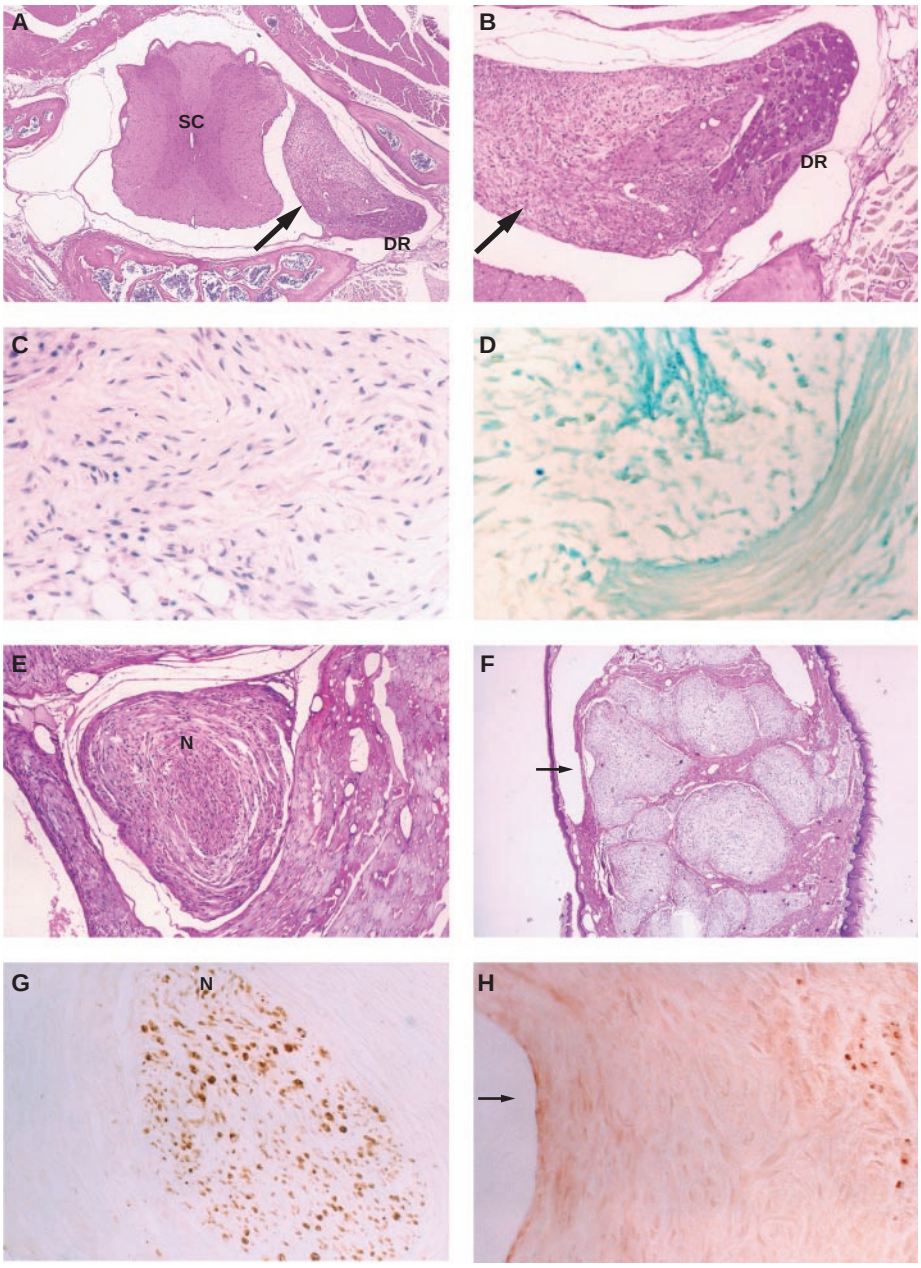

Fig. 1. Histological analysis of neurofibromas from $Nf1^{-/-}$:$Nf1^{+/+}$ chimeras. (**A** and **B**) Sections through the spinal cord (SC) and dorsal root (DR) or limb muscle (**C**) from different $Nf1^{-/-}$:$Nf1^{+/+}$ chimeric mice were stained with H+E. (B) Higher magnification of (A). Arrows in (A) and (B) indicate the neoplastic region. The entire field is composed of neoplastic tissue in (C). (**D**) Tissues from $Nf1^{+/+}$:$Nf1^{-/-}$; $ROSA\text{-}26^{+/-}$ mice were stained with X-Gal as described in (*31*). Sections of muscle (**E**) and tongue (**F**) were stained with H+E. A nerve (N) is seen in the center of the neurofibroma in (E). The neurofibroma in the tongue shown in (F) is multinodular and a portion of it identified by the arrow is also shown in (H). (**G** and **H**) Sections adjacent to (E) and (F) (higher magnification) were stained with an antibody recognizing the S100 protein.

[1]Department of Biology and Center for Cancer Research and [6]Howard Hughes Medical Institute, Massachusetts Institute of Technology, Cambridge, MA 02139, USA. [2]Merck & Co., Whitehouse Station, NJ 08889, USA. [3]Breast Center, Baylor College of Medicine, One Baylor Plaza, MS 600, Houston, TX 77030, USA. [4]Brigham and Women's Hospital, Department of Pathology, Boston, MA 02115, USA. [5]Department of Pathology, Tufts University Schools of Medicine and Veterinary Medicine, Boston, MA 02111, USA.

*These authors contributed equally to this work.
†To whom correspondence should be addressed. E-mail: tjacks@mit.edu

tiple tumors (10 to 100 per mouse), which usually emanated from the dorsal root ganglia (Fig. 1, A and B) or peripheral nerves in the limbs (Fig. 1C). Notably, only plexiform neurofibromas (those growing along the plexus of internal peripheral nerves) were observed; dermal neurofibromas, which are more common in NF1 patients, were not detected. Histologically, the lesions exhibited the classic features of human neurofibromas (*15*). Most tumors were not visible macroscopically; thus, the number of tumors per animal was probably underestimated. In two chimeras, however, tumors on the trigeminal nerve and in the tongue were visible upon dissection.

The contribution of $Nf1^{-/-}$ cells in the neurofibromas in these mice was assessed by using $Nf1^{-/-}$ ES cells containing a β-galactosidase (β-gal) expressing transgene (*16*). Five chimeras were produced with these cells. Two of the three highly chimeric animals developed multiple neurofibromas. In all cases, near uniform β-gal expression was observed in the tumors, demonstrating extensive contribution of $Nf1^{-/-}$ cells (Fig. 1D). We have not detected significant recruitment of wild-type cells into these lesions as might have been expected given the multicellular nature of human neurofibromas (see below). However, the sensitivity of 5-bromo-4-chloro-3-indolyl β-D-galactopyranoside (X-Gal) staining is not sufficient to rule out a low-level contribution of wild-type cells in this model.

Human neurofibromas contain a variety of cell types found in normal peripheral nerve including Schwann cells, perineurial cells, fibroblasts, and neurons (*15*). We used electron microscopy (EM) to determine the cellular constituents of the lesions in this mouse model. Figure 2A illustrates the overall ultrastructural appearance of a neurofibroma in this model. As in human neurofibromas Schwann cells were the most common cell type present (Fig. 2, B and C). Importantly, Schwann cells (or their precursors) are believed to be the initiating cell type [the cell type that undergoes loss of heterozygosity (LOH)] in human tumors. Cells exhibiting features of perineurial cells were also observed by EM (Fig. 2D). Taken together with the histological analysis, these data demonstrate a close similarity between the lesions in $Nf1^{-/-}$:$Nf1^{+/+}$ chimeras and human neurofibromas.

These lesions were further characterized by immunohistochemistry with an antibody recognizing S100, a protein expressed in mature Schwann cells and in most human neurofibromas and MPNSTs (*17*). As illustrated by the tumor shown in Fig. 1, E and G, S100-positive Schwann cells were observed exclusively associated with entrapped nerves (center) and were not found in the surrounding neoplastic tissue. In larger tumors in which the original nerve was disrupted (for example, Fig. 1, F and H), sparse S100 staining, associated with nerve remnants in the center of the lesion, were occasionally observed (Fig. 1H, right). In all cases ($n = 25$), only minimal S100 staining was observed in the lesion itself. The presence of S100-negative Schwann cells in the neurofibromas may be explained by their development within this model system, in which $Nf1^{-/-}$ cells are introduced at an early developmental stage (equivalent to E3.5). It is possible that the absence of S100 expression in these neurofibromas reflects a requirement for *Nf1* function in the differentiation of neural crest–derived precursors to S100-expressing Schwann cells in vivo. Indeed, neurofibromin is expressed early in Schwann cell differentiation in the mouse, 2 to 3 days before the onset of S100 expression (*18*). In contrast, in NF1 patients, neurofibromas arise from cells that are initially heterozygous for an *NF1* mutation. Cells within the human neurofibromas would be expected to become $NF1^{-/-}$, but in many cases this might occur after the onset of S100 expression, accounting for the high percentage of S100-positive neurofibromas in humans.

We next addressed the development of MPNSTs. Because these malignant tumors are often found emanating from primary plexiform benign lesions (*2, 15*), it is thought that additional (probably genetic) events are involved in the progression to malignancy. In fact, mutations in the *p53* tumor suppressor gene have been detected in human MPNSTs and therefore have been implicated in this progression step (*19*). As a means of creating a model for MPNST formation and establishing a causal role for *p53* mutations in the malignant lesions, mice with germ line mutations in *Nf1* and *p53* were generated on a mixed (129/sv × C57BL/6) genetic background. Because *Nf1* and *p53* are linked on chromosome 11 in mice (*20*), we initially generated animals carrying the *Nf1* and *p53* mutations on opposite chromosomes (NP trans) by crossing $Nf1^{+/-}$ and $p53^{+/-}$ mice. We also crossed these NP trans animals to wild-type animals to generate mice with both mutations on chromosome 11 (NP cis), which arise after meiotic recombination. Because complete chromosomal loss is the most common mutational mechanism by which second-hit mutations occur in mice (*21*), we expected most of these NP trans mice to undergo LOH at either the *Nf1* or the *p53* locus (but not both); we also thought this population of mice would exhibit a tumor phenotype reminiscent of the $Nf1^{+/-}$ and $p53^{+/-}$ parental animals (*10, 22*). In the NP cis mice, however, a chromosomal loss would be expected to result in LOH at both

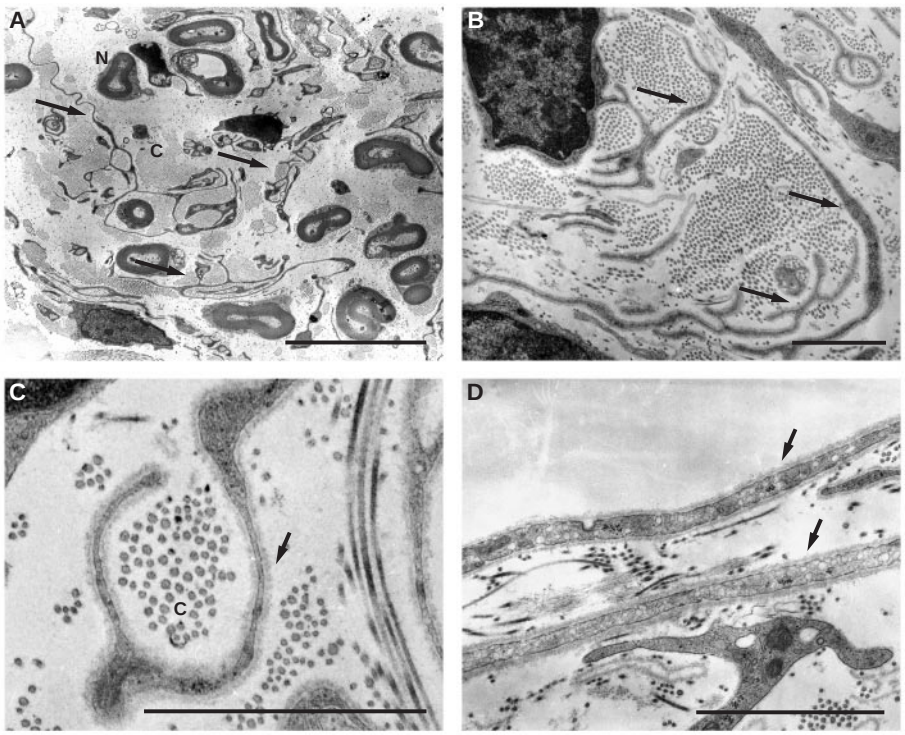

Fig. 2. Electron micrographs of murine neurofibromas. EM was performed on fixed tissue stained with lead citrate. (**A**) Low-power magnification of a neurofibroma containing myelinated axons (N), collagen bundles (C), and dissociated Schwann cells identified by arrows. Bar = 10 μm. Dissociated Schwann cells exhibit branching cytoplasmic processes (**B**) and surround collagen bundles (**C**). Note the continuous basal lamina (arrow) characteristic of Schwann cells. Bars = 1 μm. (**D**) Perineurial cells aligned in parallel arrays containing multiple pinocytotic vesicles and a basal lamina were also observed in murine neurofibromas. Cells exhibiting either discontinuous or continuous basal lamina (arrows) were observed in these tumors. Bar = 1 μm.

tumor suppressor loci simultaneously (a phenomenon we term co-LOH), resulting in cells deficient for both *Nf1* and *p53*.

As expected, NP trans animals succumbed to tumors more rapidly than mice heterozygous for a single mutation; they survived an average of 10 months and developed tumors similar to those found in mice with either single mutation (Fig. 3A). Southern blot analysis of tumor DNA ($n = 6$) revealed LOH of either the wild-type *Nf1* locus or the wild-type *p53* locus (*23*). In contrast, mice carrying *Nf1* and *p53* mutations in cis survived an average of only 5 months and exhibited a significant increase in the percentage of soft tissue sarcomas compared with mice of other genotypes ($Nf1^{+/-}$, 5%; *p53*, 57%; NP trans, 36%; NP cis, 81%). Furthermore, although NP trans animals exclusively develop osteo-, fibro-, rhabdomyo-, and hemangiosarcomas, about 30% of tumors from the NP cis animals stained positively for S100 and exhibited classic histological features of MPNSTs ($n = 28$) (Fig. 3B). The percentage of MPNSTs identified by these criteria is likely to be an underestimate because only 50% of human MPNSTs are S100-positive and due to the characteristic heterogeneity of this tumor type (*15, 24*). Importantly, loss of both wild-type alleles in tumors from the NP cis mice was consistently observed ($n = 12$) (*23*), which suggests that the loss of both genes cooperates in formation of these lesions in mice and supports a causal role for p53 mutations in development of MPNSTs in NF1 patients. The presence of S100-positive cells in the tumors from the NP cis mice contrasts with the analysis of neurofibromas in the model described above, where the lesions were universally $S100^-$. Although this pattern was unexpected, it supports the hypothesis that the timing of *Nf1* deficiency may be critical for expression of the S100 marker. Specifically, in contrast to the neurofibroma model, in the MPNSTs $Nf1^{-/-}$ cells arise from $Nf1^{+/-}$ cells, most likely at a later stage of gestation or in the adult mouse.

In summary, our data on the $Nf1^{-/-}$:$Nf1^{+/+}$ chimeras indicate that complete loss of *Nf1* is an obligate step in neurofibroma development and suggest that the prevalence of neurofibromin-deficient cells in the developing nerve is the rate-limiting factor in formation of this tumor in the mouse. It remains unclear why fewer of these cells arise in $Nf1^{+/-}$ mice than in human NF1 patients. Possible explanations include interspecies differences in lifespan, target cell number, or proliferative properties or interspecies differences in the mutability of the *NF1* locus. We have also demonstrated that mutations in *Nf1* and *p53* cooperate in the development of MPNSTs, which supports a causal role for p53 mutations in their formation. The development of these lesions might call into question the conclusion that a low rate of *Nf1* LOH limits the development of neurofibromas in $Nf1^{+/-}$ mice (see above). We hypothesize that the concomitant loss of *p53* and *Nf1* function that occurs in development of MPNSTs in the NP cis mice allows for the outgrowth of cells that otherwise would have undergone growth arrest or apoptosis were *Nf1* mutated alone. Previous work has shown that dysregulation of the Ras pathway in rat Schwann cells leads to growth arrest that can be overcome by inhibition of p53 function (*25*); oncogenic *ras* alleles can also induce p53-dependent growth arrest or apoptosis in human and mouse fibroblasts (*26*).

The simultaneous homozygosing of linked mutations by the process described here as co-LOH could have more general importance in tumor development, which could be strongly influenced either positively or negatively by the arrangement of linked germ line or somatically acquired mutations.

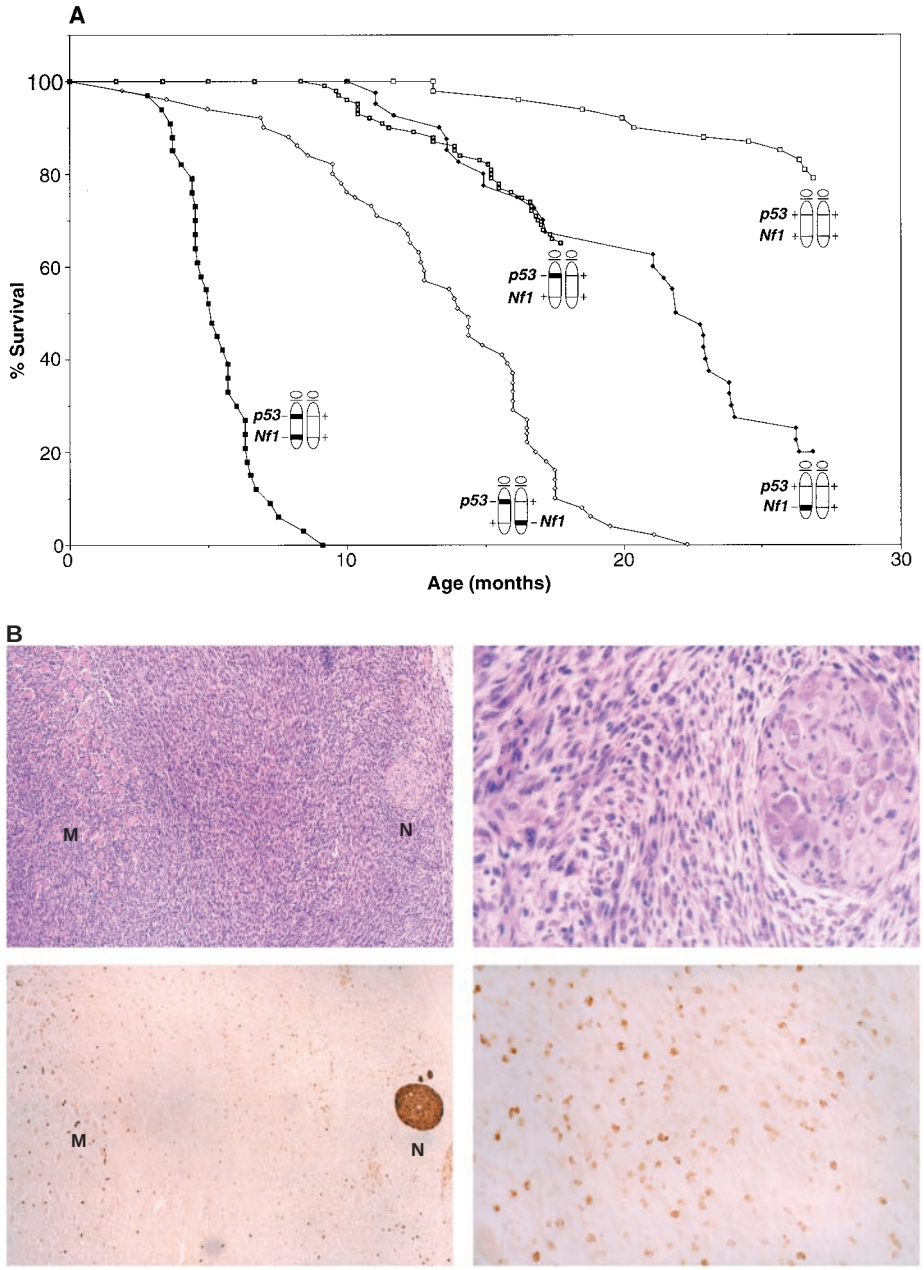

Fig. 3. Analysis of $Nf1^{+/-}$:$p53^{+/-}$ mice. (**A**) Survival curve of mice carrying *Nf1* and *p53* mutations on the same (NP cis) or opposing (NP trans) chromosomes. The $Nf1^{+/-}$ and $p53^{+/-}$ curves are identical to those published previously. We studied 51 NP trans animals, 34 NP cis animals, 19 wild-type animals, 37 $Nf1^{+/-}$ animals, and 41 $p53^{+/-}$ animals. (**B**) Sections of an MPNST arising in the rear flank of this animal were stained with H+E (upper) or S100 antibodies (lower). The nuclear S100 staining observed is also a characteristic of human MPNSTs and neurofibromas. MPNSTs were typically observed invading muscle (M) and were associated with nerves (N). Right panels are magnified views of left panels.

This effect may be more pronounced in mice than in humans, where LOH events are typically subchromosomal. Still, closely linked mutations that act synergistically or antagonistically could strongly affect the process of human tumor development through this mechanism.

Finally, we anticipate that both models will be critical in further characterization of tumorigenic mechanisms in NF1 and in the evaluation of potential therapies, such as compounds designed to inhibit Ras signaling, such as farnesyl transferase inhibitors (*27*).

References and Notes

1. D. A. Stumph, *Arch. Neurol.* **45**, 575 (1987).
2. V. M. Riccardi, *Neurofibromatosis: Phenotype, Natural History, and Pathogenesis* (Johns Hopkins Univ. Press, Baltimore, ed. 2, 1992).
3. J. L. Bader, *Ann. N.Y. Acad. Sci.* **486**, 57 (1986); D. G. Hope and J. J. Mulvihill, *Adv. Neurol.* **29**, 33 (1981).
4. R. M. Cawthon *et al.*, *Cell* **62**, 193 (1990); D. Viskochil *et al.*, *Cell* **62**, 187 (1990); M. R. Wallace *et al.*, *Science* **249**, 181 (1990).
5. G. A. Martin *et al.*, *Cell* **63**, 843 (1990); G. F. Xu *et al.*, *Cell* **63**, 835 (1990).
6. T. N. Basu *et al.*, *Nature* **356**, 713 (1992); G. Bollag *et al.*, *Nature Genet.* **12**, 144 (1996); E. DeClue *et al.*, *Cell* **69**, 265 (1992); A. Guha *et al.*, *Oncogene* **12**, 507 (1996).
7. K. M. Shannon *et al.*, *N. Engl. J. Med.* **330**, 597 (1994); E. Legius, D. A. Marchuk, F. S. Collins, T. W. Glover, *Nature Genet.* **3**, 122 (1993); W. Xu *et al.*, *Genes Chromosomes Cancer* **4**, 337 (1992).
8. S. D. Colman, C. A. Williams, M. R. Wallace, *Nature Genet.* **11**, 90 (1995); S. Sawada, *et al.*, *Nature Genet.* **14**, 110 (1996).
9. K. Daschner *et al.*, *Biochem. Biophys. Res. Commun.* **234**, 346 (1997); T. W. Glover *et al.*, *Genes Chromosomes Cancer* **3**, 62 (1991); R. A. Lothe *et al.*, *J. Neuropathol. Exp. Neurol.* **54**, 65 (1995); M. Stark, G. Assum, W. Krone, *Hum. Genet.* **96**, 619 (1995).
10. T. Jacks *et al.*, *Nature Genet.* **7**, 353 (1994).
11. C. I. Brannan *et al.*, *Genes Dev.* **8**, 1019 (1994).
12. *Nf1*$^{-/-}$ ES cells were generated with a two-step targeting strategy (*28*). D3-derived ES cell lines containing a disruption of one *Nf1* allele with a neomycin (*neo*) resistance gene replacing exon 31 have been described (*10*). These cells were retargeted with a second vector containing a hygromycin resistance gene in place of the *neo* gene, and two *Nf1*$^{-/-}$ lines (designated clones 6 and 47) were identified after selection in G418 and hygromycin. Mutations in both *Nf1* alleles were confirmed by Southern blot analysis as described in (*10, 21*).
13. Supplementary material is available at www.sciencemag.org/feature/data/1043163.shl.
14. Tissues were dissected, fixed in 10% formalin or Bouin's fixative and dehydrated in graded alcohol solutions. Paraffin-embedded tissues were cut in 4-μm sections and stained with hematoxylin and eosin (H+E).
15. J. M. Woodruff, in *Soft Tissue Tumors* (International Academy of Pathology, Baltimore, 1996).
16. *Nf1*$^{+/-}$ animals were crossed to mice carrying a β-gal transgene driven by the ubiquitously expressing *ROSA-26* promoter (*29*). *Nf1*$^{+/-}$, *ROSA-26*$^{+/-}$ ES cells were then generated de novo from delayed blastocysts (*30*), and the second *Nf1* allele was retargeted by using the hygromycin targeting construct used to generate the previous *Nf1*$^{-/-}$ cell lines (*12*).
17. Tissues were fixed in 10% formalin and processed as described. Immunohistochemical analysis using an S100 antibody (Dako) was done according to the manufacturer's instructions.
18. C. Kioussi and P. Gruss, *Trends Genet.* **12**, 84 (1996); D. H. Gutmann, J. L. Cole, F. S. Collins, *Prog. Brain Res.* **105**, 327 (1995).
19. A. G. Menon *et al.*, *Proc. Natl. Acad. Sci. U.S.A.* **87**, 5435 (1990); M. S. Greenblatt, W. P. Bennett, M. Hollstein, C. C. Harris, *Cancer Res.* **54**, 4855 (1994).
20. A. M. Buchberg, M. S. Buckwalter, S. A. Camper, *Mammalian Genome* **3**, S162 (1992).
21. C. Luongo, A. R. Moser, S. Gledhill, W. F. Dove, *Cancer Res.* **54**, 5947 (1994).
22. T. Jacks *et al.*, *Curr. Biol.* **4**, 1 (1994); L. A. Donehower *et al.*, *Nature* **356**, 215 (1992).
23. Supplementary material is available at www.sciencemag.org/feature/data/1043163.shl.
24. M. R. Wick, P. E. Swanson, B. W. Scheithauer, J. C. Manivel, *Am. J. Clin. Pathol.* **87**, 425 (1987).
25. A. J. Ridley, H. F. Paterson, M. Noble, H. Land, *EMBO J.* **7**, 1635 (1988).
26. A. W. Lin *et al.*, *Genes Dev.* **12**, 3008 (1998); M. Serrano, A. W. Lin, M. E. McCurrach, D. Beach, S. W. Lowe, *Cell* **88**, 593 (1997); M. S. Soengas *et al.*, *Science* **284**, 156 (1999).
27. J. B. Gibbs, A. Oliff, N. E. Kohl, *Cell* **77**, 175 (1994).
28. H. te Riele, E. R. Maandag, A. Clarke, M. Hooper, A. Berns, *Nature* **348**, 649 (1990).
29. G. Friedrich, P. Soriano, *Methods Enzymol.* **225**, 681 (1993).
30. E. J. Robertson in *Teratomas and Embryonic Stem Cells: A Practical Approach,* E. J. Robertson, Ed. (IRL Press, Oxford 1987), pp. 71–112.31.
31. A. I. McClatchey, I. Saotome, V. Ramesh, J. F. Gusella, T. Jacks, *Genes Dev.* **11**, 1253 (1997).

32. We thank D. Anthony, C. Fletcher, D. Housman, and M. Entman for helpful discussions and K. Mercer and D. Crowley for assistance with histology. K.C. was supported by an NNFF Young Investigator Award. This work was supported in part by a grant from the Department of the Army and the Medallion Foundation.

1 July 1999; accepted 14 October 1999

Mouse Tumor Model for Neurofibromatosis Type 1

Kristine S. Vogel,[1]*† Laura J. Klesse,[1]* Susana Velasco-Miguel,[1]* Kimberly Meyers,[1]* Elizabeth J. Rushing,[2] Luis F. Parada[1] ‡

Neurofibromatosis type 1 (NF1) is an autosomal dominant disorder characterized by increased incidence of benign and malignant tumors of neural crest origin. Mutations that activate the protooncogene *ras*, such as loss of *Nf1*, cooperate with inactivating mutations at the *p53* tumor suppressor gene during malignant transformation. One hundred percent of mice harboring null *Nf1* and *p53* alleles in cis synergize to develop soft tissue sarcomas between 3 and 7 months of age. These sarcomas exhibit loss of heterozygosity at both gene loci and express phenotypic traits characteristic of neural crest derivatives and human NF1 malignancies.

Mutations in tumor suppressor genes are common events in human cancers (*1*). Individuals with a mutation in one copy of the *NF1* gene develop benign cutaneous neurofibromas, plexiform neurofibromas, café-au-lait spots, and axillary freckling (*2*). Through loss of heterozygosity (LOH) at the *NF1* locus, patients with neurofibromatosis type 1 are at increased risk of developing malignancies of neural crest derivatives, including malignant peripheral nerve sheath tumors (MPNSTs), malignant Triton tumors (MTTs), and pheochromocytomas (*2, 3*). MPNSTs and MTTs arise from plexiform neurofibromas and frequently are associated with mutation or loss of the *p53* tumor suppressor gene (*2, 4*). The protein product of the *NF1* gene neurofibromin is a guanosine triphosphatase (GTPase)–activating protein (GAP) that can negatively regulate p21ras signaling (*5*). Mutations that activate Ras cooperate with mutations that inactivate p53 in a number of transformation assays and models of tumorigenesis (*6*).

The *Nf1* and *p53* genes are linked in humans and in mice (*7*). To determine whether null mutations in *Nf1* and *p53* cooperate to accelerate tumorigenesis in vivo, we generated a recombinant mouse strain harboring inactivated *Nf1* and *p53* alleles linked on mouse chromosome 11. We accomplished this with intercrosses of trans-Nf1$^{+/-}$:p53$^{+/-}$ compound heterozygotes or through crosses with p53$^{+/-}$ heterozygotes. The integrity of the recombinant cis-Nf1:p53 chromosome was established by genomic Southern blot analysis and by polymerase chain reaction (PCR). All progeny of cis-Nf1$^{+/-}$:p53$^{+/-}$ test crosses to wild-type animals were either compound heterozygotes or entirely wild type, which confirms the integrity of the double-mutant chromosome.

Mice that are heterozygous for the *Nf1* mutation alone are at increased risk of developing pheochromocytomas and myeloid leukemias between 18 and 28 months of age (*8*). Loss of one or both copies of the *p53* gene leads to accelerated tumorigenesis. Thus, p53$^{-/-}$ mice develop lymphomas and hemangiosarcomas by 6 months of age, whereas p53$^{+/-}$ mice exhibit a predominance of osteosarcomas that arise later, after 9 months (*9*). We compared the mortality of trans- and cis-Nf1$^{+/-}$:p53$^{+/-}$ compound heterozygotes with that of p53$^{+/-}$ and

[1]Center for Developmental Biology and [2]Department of Pathology, University of Texas Southwestern Medical Center, 6000 Harry Hines Blvd., Dallas, TX 75235–9133, USA.

*These authors contributed equally to this work.
†Present address: Department of Cell Biology and Anatomy, Louisiana State University Medical Center, New Orleans, LA 70112, USA.
‡To whom correspondence should be addressed. E-mail: parada@utsw.swmed.edu